

SOME REMARKS ABOUT CHEMICAL PRESTRESSING OF FRP REINFORCEMENT

V. V. Tur

Doctor of Technical Sciences, Professor, Head the Department of Concrete Technology and Building Materials, Brest State Technical University, Brest, Belarus, e-mail: profvturvic@gmail.com

Abstract

In last years has been observed a new wave of interest in the research and practical use of self-stressing concrete, now in combination with various types of non-traditional reinforcement. One of the widely used types of these reinforcements is FRP bars and long fibers (textile). We connect the major problems of FRP reinforcement using as a structural reinforcement with the development of exceeding deflections as well as crack opening under service loads. One of the most effective methods for its performance enhancing is chemical pre-stressing with self-stressing concrete. When self-stressing concrete matrix combined with textile forms a new composite material, namely according to Boxing Wang et al., textile-reinforced self-stressing concrete (TRSSC). This paper presents a critical analysis of some basic assumptions of the proposed models for assessment restraint strains/self-stresses distribution and calculation method of cracking load and deflection of textile reinforced self-stressing concrete.

Keywords: self-stressing concrete, FRP reinforcement, textile, restraint strain.

НЕКОТОРЫЕ ЗАМЕЧАНИЯ О ХИМИЧЕСКОМ ПРЕДВАРИТЕЛЬНОМ НАПРЯЖЕНИИ КОМПОЗИТНОЙ АРМАТУРЫ

В. В. Тур

Реферат

В последние годы наблюдается новая волна интереса в исследованиях и практическом применении напрягающего бетона, теперь в сочетании с нетрадиционными видами армирования. Одним из наиболее широко применяемых видов армирования считается композитная арматура и т.н. текстильные материалы на основе длинной фибры, применяемой в полимерных композитах. Главная проблема, связанная с применением таких материалов связана с чрезмерной шириной раскрытия трещин и развитием прогибов при действии эксплуатационных нагрузок. Одним из наиболее эффективных методов повышения эксплуатационных свойств конструкций армированных полимерными композитами является самоупрочнение при использовании для этого напрягающего бетона. Напрягающий бетон в комбинации с текстильными материалами позволяет получить новый, по мнению Б. Ванга, строительный материал (TRSSC). В статье представлен критический анализ некоторых базовых положений расчётных моделей, предложенных Вангом для оценивания связанных деформаций и самоупрочнений, а также моделей трещиностойкости и прогибов.

Ключевые слова: напрягающий бетон, композитная арматура, текстиль, связанная деформация.

Theory is when you know everything and *nothing* works; *practice* is when everything works and nobody knows why. Here we combine theory with practice: nothing works and nobody knows why.
Albert Einstein

Introduction

The main reason for this paper writing is my long-term interest in expansive cement, self-stressing concrete and self-stressed structures. Over 40 years I work with this unusual material and such type of pre-stressed structure in the research laboratory and at the building site. In various time periods, interest and assessments of the self-stressing concrete were very different: from admiration after its successful utilization in the civil engineering works (for instance, joint less self-stressed/post-tensioned slab-on-grade with size 144x72m) to great criticism and sarcasm when shrinkage cracking appeared after full pre-stressing loosening or even self-damaging taking place in case for "unbalanced" expansion and strength development. In recent years number of publications dedicated to self-stressing and shrinkage-compensating concrete utilization increased sufficiently (from steel fibre concrete to textile-reinforced self-stressing concrete) and sometimes I can only briefly read a new article related to this issue. Among very interesting and fundamental research works, which show a very high scientific level (for example, Ito et al.) and open new horizons of practical utilization of the expansive composites, we can meet papers with very controversial individual statements or full content.

In this paper, I want to pay attention to the most controversial series of articles [10–12] dedicated to textile-reinforced self-stressed concrete (TRSSC), mainly the "Theory of self-stressing distribution models" and experimental results used for verification of these models. At the beginning, we have to tell some words about textile-reinforced concrete. In recent decades, it has developed various ways to replace conventional reinforcing steel (short fibre concrete, various type of FRP-reinforced concrete). Consideration to replace steel reinforcement by use of continuous fibres or grids that were made from continuous fibres began in the 1980s [18]. Among experts, *this new, innovative composite building*

material is known today as *textile-reinforced concrete* (TRC). The mechanical and material properties of TRC have been extensively investigated [18]. In investigations [10–12] "self-stressing concrete (SSC) matrix was combined with textile to form a new composite material, namely, textile-reinforced self-stressing concrete (TRSSC). In this material, textile functions as expansion confinements to SSC to attain self-stress."

In the analysis process, we will pay attention to some statements from other articles related to this topic (for example, the priorities of expansive cement or self-stressing models development), which we are considered as not fully correct. Considering some important data (for instance, the 120-years Anniversary of prof. V.Mikhailov), I think that brief historical background will be useful.

1. Brief Historical review

Intensive development of the Portland cement concrete technology in the last decades allowed to obtain high-performance concrete (HPC) or even ultra-high performance concrete (UHPC) with a compressive strength above 120 MPa. Nevertheless, the inadequate ratio of any concretes compressive to tensile strength (as it was stated in our works [15–17], concretes of the new generation are still artificial stones with good performance under compression-only). Low tensile strength in combination with inherent to concrete early-age and long-term effects (autogenous as well as drying shrinkage, creep, temperature) lead to decreasing of the serviceability parameters of concrete structures. For instance, restrained shrinkage and temperature deformations lead to the additional tensile stresses appearance in the concrete structure causing cracks (cracks of varying sizes can be found in practically every reinforced concrete structures). Obviously, such cracking of concrete reduces structural durability in general. Based on the sustainable development strategy, *fib* Symposium 2020 in China defines concrete of the new generation as a High-durability concrete (HDC). To permit a more efficient utilization of structural concrete, the search for means of overcoming these weaknesses had led to mechanical pre-stressing of steel tendons. By keeping the concrete in compression, cracking is prevented. In the general case, mechanical pre-stressing requires elaborate equipment and techniques.

Considerable advantage can be derived from concrete which is expanding under the varying types of restraint induces a restrained strain and, as a result compressive pre-stress of sufficient magnitude to compensate for shrinkage effect (so-called shrinkage compensating concrete), or induces compressive stresses a high enough magnitude to result in significant compression in the concrete after autogenous and drying shrinkage has occurred (self-stressing concrete). The above-mentioned problem led to the idea of the physico-chemical (or sometimes called chemical) method of concrete structures volume pre-stressing. In 1953 I. Giyon wrote in his monograph: "In case we reached a significant restrained expansion of the concrete that could provide an adequate reinforcement pre-tensioning, without doubts, we will get a principally new method of the beams pre-stressing".

The history of the development of expansive cement (self-stressing and shrinkage-compensating concrete) application counts for about 90 years and can be said to have originated from an investigation of ettringite in cement. Ettringite ($3\text{CaO} \cdot \text{Al}_2\text{O}_3 \cdot 3\text{CaSO}_4 \cdot 32\text{H}_2\text{O}$) – is the phase formed during hydration of expansive cements which is the source of the expansion force. It is comparable to the natural mineral of the same name. This high sulfate calcium sulfoaluminate is also formed by sulfate attack on mortar and concrete (delayed ettringite) and was defined as "cement bacillus" in older literature. Candlot [1] reported in 1890 that this product resulted from reaction of ticalcium aluminate (C_3A) with calcium sulfate (CaSO_4). Michaelis [2] in 1892 suggested that ettringite was responsible for destructive expansion of Portland cement concretes in the presence of environmental containing sulfates.

One of the earliest investigators to recognize the potential of ettringite in the elimination of shrinkage and possibly of inducing pre-stress was Henry Lossier [3]. His works extended more than 20 years, starting in the mid-1930s and the cement he develops consisted of Portland cement, an expansive component (grinding gypsum, bauxites, and chalk to slurry burning the mixture to a clinker) and blast furnace slag.

Russian work by prof. V.Mikhailov [4, 5] in field of expansive cement followed two different courses to obtain an expansive cement to repairs and waterproofing and self-stressing cement. Expansive cement type M – is either a mixture of Portland cement, calcium aluminate cement and calcium sulfate or an inter-ground product made with Portland cement clinker, calcium aluminate clinker and calcium sulfate. In monograph [5], we can find the first formulation of the solid-state or solid-phase expansion mechanism of the matrix as a fundamental condition of concrete self-stressing under restraint and the related requirement to the expansive cement composition (for instance, the ratio $\text{Al}_2\text{O}_3/\text{SO}_3$ in a binder and expansive component).

Studies by Klein [7,8] and his associates at the University of California are based on the formation of a stable anhydrous calcium sulfoaluminate compound by heat treating a mixture of bauxite, chalk, gypsum at about 2400F. While the ingredients were quite similar to those used in the Lossier cements, the material selection and clinking conditions probably contributed to the formation of an anhydrous calcium sulfoaluminate, calcium sulfate and lime, produced a cement that could be handled much in the same manner as a regular cement and adjusted to offset shrinkage and produce large net expansion [9]. In recent years, some new types of the expansive cement and expansive additives to OPC are proposed, but all these materials based on the reaction of the ettringite formation (CSA-type). It should be mentioned that besides the use of expansive potential generated by ettringite formation, another type of expansive admixtures takes use of hydroxide formation. As well, periclase has been employed in dam construction as the expanding agent in China.

Therefore, it is strange to read the following statement from the one article: "Calcium sulfoaluminate cements have essentially been developed in China in 1970s"

At the beginning, after a short historical review I want briefly to present some most popular models for self-stresses values assessment and possibility of their application to design of the self-stressed elements with FRP reinforcement.

2 Design models for estimation early-ages restrained strains and self-stresses

2.1 Short review

There are following main direction with respect to the actual design models for assessment the early-age restrained expansion strains and stresses in self-stressing concrete element under restraint conditions:

- 1) Models based on the chemical energy conservation law [4, 5, 14, 22]. Apropos, professor V. Mikhailov formulated this method first in 1972, therefore the following statement from [14] "the author (Tsuji) has proposed from some time ago a very convenient method based on conception of work quantity, and a general method for making estimations

for the cases of applying expansive concrete in reinforced concrete" is not fully correct. In this time period in SU was developed and implemented standard for self-stressed structures design [28] in which calculation method developed by V.Mikhailov was based on the energy conservation approach. On the other hand, Tsuji [14] developed a convenient practical method for estimating the strain/stress of reinforcing bars in RC members made of expansive concrete, based on the hypothesis that the quantity of work per unit volume by expansion is constant and do not include constants such as modulus of elasticity and creep coefficient of expansive concrete. In these methods, two hypotheses such as ones below are set: a) expansive strains are linearly distributed in the direction of cross-section height; b) the work quantity U that expansive concrete performs against restraint per unit volume is a constant regardless of the degree of restraint by external restraining objects. This method is more flexible and applicable for different types of self-stressed structural elements (mainly for composite beams and elements with asymmetrical longitudinal reinforcement distribution in cross-section) in comparison with the semi-empirical coefficient method [21] proposed by prof. V.Mikhajlov.

- 2) Analytical models [14-17, 23, 24]. As it was stated in [23], "there have been particularly few analytical investigations on early-age induced stress in HSC containing expansive additive. Pointing this area, Sato et al. carry out two-dimensional FE analysis based on the effective modulus method considering the principle of superposition and the age at application of load on creep in order to evaluate early-age shrinkage/expansion-induced stress in RC-beams. A comparison of computes values indicated the necessity of adopting stricter creep analysis methods and actual creep coefficients."

Fundamental approach developed by Ito et al. [23] consists of Finite element model and its practical realization as the method based on beam theory, which consider the principle of superposition and linear stress-strain relation of creep, in order to evaluate the early age shrinkage/expansion-induced stress in reinforced member. I think today it is the most progressive and perspective model for early-age self-stressing concrete strain/stress assessment. Some modification of this model for self-stressing concrete with high energy of expansion presents in our works [15-17].

- 3) Empirical exponential function models [12];
- 4) Semi-empirical models [13];

In last years, artificial neural network (ANN) and fuzzy inference system model (FIS) for predicting free expansion have been developed [20].

All listed above, models proposed for assessment early age strains/stresses in the self-stressing concrete elements are based on the following fundamental assumptions:

- (1) Self-stressing is the specific type of the mechanical pre-stressing, in which the tensile force in the tendons and equal resultant compression force in concrete are induced gradually in time as a result the work that self-stressing concrete performs against restraint;
- (2) Expansive strains are linearly distributed in the direction of cross-sectional height (plain section hypothesis is valid). In the first approximation, the cases considered are those when misalignments are not produced at the respective boundaries between expansive concrete and reinforcing bars. Based on the assumption that self-stresses in concrete are considered as the product of the *elastic strains* and modulus of elasticity $E_{cm}(t)$, at the state of stabilization of the expansion stresses are distributed linearly too.

On the other hand, the distribution of the stresses in the cross-section can be calculated as well as for the mechanically pre-stressed structure. Here, the resultant force in restraint is considered the pre-stressing force.

2.2 New Theory of self-stressing distribution model according to [10, 11]

What basic assumptions is used a new model for assessment self-stresses in TRCC according to [10, 11]? On the one hand, in article [10] we can to read the following: "Self-stress is distributed along the fibre bundle in the textile and exhibits similar effect to that of mechanical pre-stress." This statement complies with assumptions adopted in the models listed above and considered TRSSC element as the pre-stressed element. The next assumptions about stresses distributions look strange and require comments.

According to [10] analysis of cracking load is based on the following three assumptions:

- a) The beam is in elastic stage and conforms to the assumption of small deformation before cracking-(no comments)
- b) The relative displacement between matrix and the woven fabric is ignored- (no comments)
- c) The self-stress value was distributed identically within range of 5mm above and below the textile (see Fig. 1) - (need comments)

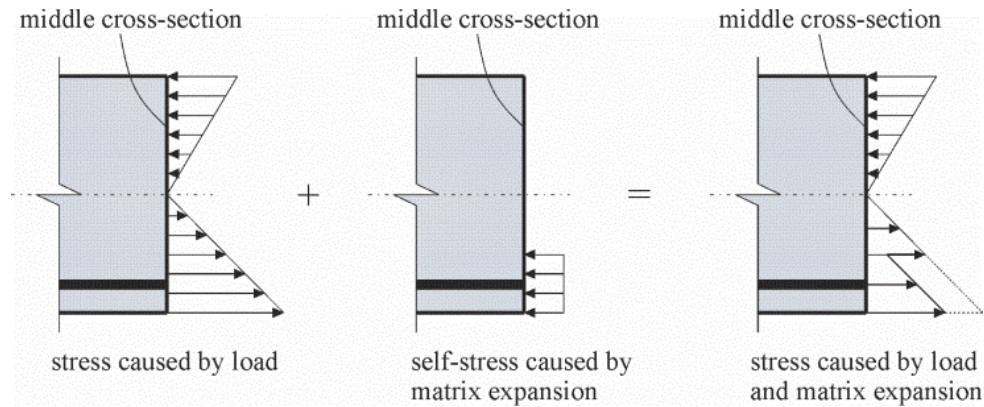


Figure 1 – Stressing distribution of TRSSC beam section according to [10]

Analysis of presented assumptions (mainly assumption c) and Figure 1 initiates following questions:

- (1) Why self-stresses are distributed identically at the local area limited within the range of 5 mm above and below the textile? (Why not 5.5mm; 7mm; 5.6 mm...? What is the influence of bundle area? What is the scientific background of this range?);
- (2) Is not valid for such new composites plain section law at the stage of expansion? Is the non-linear distribution of the strains in the section's depth in the test?
- (3) Is the rest part of the section free from self-stressing if self-stresses concentrate within a limited range above and below textile reinforcement?

Maybe, philosophy of the authors [10-12] related to self-stressing of the concrete can be explained by a following statement from article [12]: "steel bar-reinforced self-stressing concrete (SSC) and other types of reinforced SSC also have inherent shortcomings. The steel bar used to reinforce SSC cannot influence the entire concrete cross-section uniformly. Placing the concrete near steel bar could produce confinement, whereas placing the concrete far from the steel bar may cause deformation without confinement. Also, when the free expansion strain of the SSC matrix is too high, concrete located distant from the steel bar could incur cracks because **overexpansion**".

The scientific background of this last assumption (c) authors proposed to find in article [11]. What can we read in this paper?

"The expansion of self-stressing concrete matrix was restricted by the interface between the textile and the matrix; therefore, self-stress was formed, and its value varied with the section height. The compacted level was different because of varied self-stressing values on different areas; thus, the elasticity modulus was not identical. Several fundamental assumptions were suggested for self-stressing distribution model:

- (1) The self-stress value is generated because longitudinal fiber bundles resist the expansion of the matrix, and the effective range is higher than 10mm; conversely, the latitudinal bundles minimally influence the matrix expansion and is therefore neglected.
- (2) The symmetry axis of self-stress is the axle center. Self-stress value is distributed as a quadratic function along z-axis.

-
- (4) Each layer shows deformation compatibility and does not slide relatively during tensile (?) testing. The self-stressing value along the z direction is ignored."

What are we reading now? The effective range of self-stresses distribution is higher than 10mm and self-stress value is distributed as a quadratic function along z-axis. Moreover, the symmetry axis of self-stress is the axle center (of the section?). I think that looking for your answers to these questions is useless; it is easier to use the results of your research on self-stressed elements reinforced with different FRP and compare it with proposed by authors [10-12] "theory of self-stressing distribution model" and cracking resistance model.

3. Experimental studies of self-stressed element reinforced with FRP

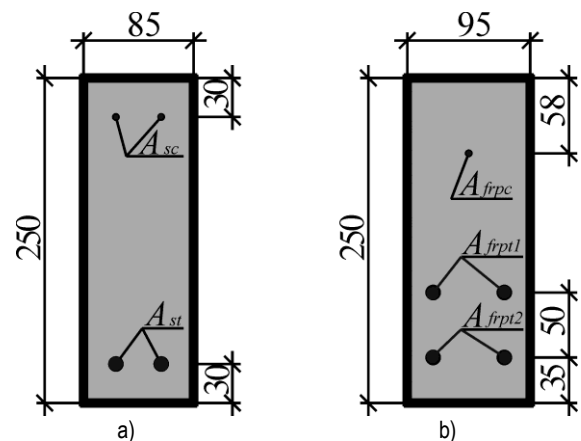
Let us consider the results of the two research works [16, 27], in which we used self-stressing concrete for beam elements reinforced with FRP bars. In the first research [16], we studied the possibility of applying self-stressing concrete to increase FRP reinforcement's effectiveness, mainly increasing crack resistance and flexural stiffness (satisfying of the

serviceability limit state requirements). We adopted the following work hypothesis: expanding of self-stressing concrete in restraint conditions developed by FRP bars induces tensile force in restraint and compression forces (self-stresses) in concrete. The relatively low axial stiffness of FRP bars allows sufficient restrained strains that cannot be fully compensated for shrinkage development. In work [16] we studied the influence of the level of got self-stresses on the crack resistance and deflection of the beam elements reinforced with FRP longitudinal bars. In the second experiment presented in [27], we investigated the shear resistance of the self-stressed elements without stirrups and reinforced them with longitudinal FRP bars (GFRP and CFRP). For evaluation of the effects related to the usage of the self-stressing concrete jointly with FRP bars in first and second cases performed self-stressed elements with steel reinforcement and elements from OPC-concrete with FRP bars.

3.1 Experimental studies [16]

3.1.1 Test specimens

Experimental studies [16] were carried out on two series of self-stressed concrete beams with different type of reinforcing bars. Experimental beams cross-section geometry with reinforcement areas and arrangement are shown in Fig. 2.



a) – self-stressed beams of the series I (I-BECS-(1...4):

$A_{sc} = 25,1 \text{ mm}^2 (2\text{Ø}4)$; $A_{st} = 157,0 \text{ mm}^2 (2\text{Ø}10)$;

b) – self-stressed beams of the series II (II-BECF-(1,2):

$A_{frpc} = 13,7 \text{ mm}^2 (1\text{Ø}4)$; $A_{frpt1} = 143,5 \text{ mm}^2 (2\text{Ø}10)$;

$A_{frpt2} = 143,5 \text{ mm}^2 (2\text{Ø}10)$; II-BECF-(3):

$A_{frpc} = 13,7 \text{ mm}^2 (1\text{Ø}4)$; $A_{frpt1} = 143,5 \text{ mm}^2 (2\text{Ø}10)$;

$A_{frpt2} = 330,5 \text{ mm}^2 (2\text{Ø}14)$)

Figure 2 – Experimental beams cross-section geometry with reinforcement areas and arrangement [17]

Expansive cement composition was consisted of the following components in the following proportions (by weight): Ordinary Portland cement (CEMI-42,5N) – 71 %; metakaolin – 14 %; gypsum ($\text{CaSO}_4 \cdot 2\text{H}_2\text{O}$) – 15 %. The main mechanical characteristics of the hardened expansive cement established in accordance with [7, 8] are presented in Table 1.

Table 1 – Expansive cement characteristics

Expansion		Strength	
free expansion strain $\epsilon_{f,i}$, %	reference self-stress $f_{CE,d}$, MPa	flexural f_{flex} , MPa	compressive f_{cm} , MPa
1,21	5,9	5,5	50,8

Notes: 1. Expansion and strength characteristics were established at the 28 days age of the mortar bars hardened in the unrestrained conditions;
2. Reference self-stress, $f_{CE,d}$ was established in standard restraint conditions: $\rho_l = 1\%$ and $E_s = 200$ GPa.

Self-stressed beams of the both series were made of self-stressing concrete with characteristics presented in Table 2.

Table 2 – Average values of the self-stressing concrete characteristics

Series	Expansion characteristics at the concrete expansion stabilization		Mechanical characteristics	
	free expansion strain $\epsilon_{CE,f}$, %	reference self-stress $f_{CE,d}$, MPa	compressive strength $f_{cm,28}$, MPa	modulus of elasticity $E_{cm,28}$, GPa
I	0,47	2,4	33,2	25,3
II	0,55	2,8	37,8	25,7

Notes: 1. Free expansion strain, $\epsilon_{CE,f}$, was established on the unrestrained specimens;
2. Reference self-stress, $f_{CE,d}$ was established in the standard restraint conditions: $\rho=1\%$ and $E_s=200$ GPa;
3. Modulus of elasticity was established on the cylindrical specimens ($\varnothing=150$ mm, $h=300$ mm).

Steel and FRP reinforcing bars characteristics are listed in Table 3 and Table 4.

Table 3 – Average values of the mechanical characteristics of steel reinforcing bars (experimental values)

Nominal diameter, mm	Yield stress f_{ym} , MPa	Modulus of elasticity E_{sm} , GPa
4	573,2	200,0
10	625,7	

Table 4 – Average values of the mechanical characteristics of FRP reinforcing bars (experimental values)

Nominal diameter, mm	Type of fibers	Modulus of elasticity E_{frpm} , GPa	Tensile strength f_{frpm} , MPa	Ultimate tensile strain ϵ_{frpm} , %
5	Basalt	51,5	1262	2,45
10	Glass	45,2	1027	2,27
14	Glass			

3.1.2 Results of experimental research

3.1.2.1 Self-stressing stage, restrained strains distribution

Experimental values of the restrained strains and self-stresses in concrete on the depth of the cross-section gravity center immediately before static loading are listed in the Table 5.

Table 5 – Experimental values of restrained strains and self-stresses immediately before static loading

Unit code	Restrained strains, [%]			Self-stress σ_{CE} , [MPa]
	$\sum(\Delta\epsilon_{CE,i})_i$	$\sum(\Delta\epsilon_{CE,m})_i$	$\sum(\Delta\epsilon_{CE,b})_i$	
I-BECS-(1)	0,342	–	0,128	2,69
I-BECS-(2)	0,372	–	0,144	2,95
I-BECS-(3)	0,443	–	0,144	3,00
I-BECS-(4)	0,499	–	0,154	3,46
II-BECF-(1)	0,481	0,330	0,269	1,78
II-BECF-(2)	0,556	0,365	0,276	1,92
II-BECF-(3)	0,429	0,267	0,197	2,10

As shown in Table 5, in all the tested beams, the initial value of self-stresses was got in the range from 1,8 to 3,5 MPa depending on the reinforcing bars' type, area, and arrangement. Reached pre-tensioning in reinforcing bars were at average 46 % from yield strain and 14 % from

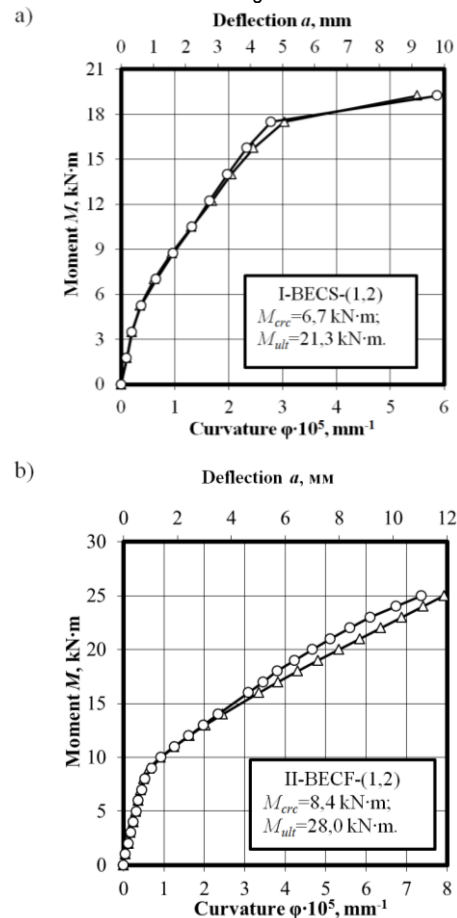
ultimate tensile strain for steel and FRP reinforcing bars respectively. It should be pointed that for the members pre-stressed with FRP reinforcing bars in accordance with [9], initial values of the pre-stress should be limited by the 24 % from the ultimate tensile strength.

Beams initial restrained expansion curvature values obtained on the basis of measured restrained strains and measures deflections varied in the diapason $(1,16-1,82) \cdot 10^{-5} \text{ mm}^{-1}$ and $(3,7-4,1) \text{ mm}$ respectively. These values of the initial restrained expansion curvature of the beams got at the self-stressing stage should be considered because two developed in time-superposed basic processes: (1) on the one hand—self-stressing concrete expansion in asymmetrical restraint conditions and (2) on the other hand—concrete elastic compressive strains accumulating under monotonically increasing in time restraint reaction [1, 5, 6]. It should be pointed that plane section hypothesis was valid for all tested beams. The so-called beam initial «elastic» curvature (that is determined from the accumulated concrete elastic compressive strains distribution) only have an influence on the self-stressed member behavior under the applied static load in terms of traditional decompression. In contrast with traditional pre-stressed members, in the self-stressed members the values of the beam initial «elastic» curvature is not possible to establish based on the direct strains measurement, but it can be obtained under the proposed MSDM concept [1, 2].

3.1.2.2. Load-deflection responses and failure modes

After the self-stressing concrete expansion stabilization was reached, self-stressed beams were tested with monotonically increasing load by means of two concentrated forces applied at the 1/3 and 2/3 points of the 1200 mm span. The main aim of the static loading consisted in the investigation of the influence of the achieved initial stress-strain state obtained to the self-stressing concrete expansion stabilization on the behavior of the tested beams under the load.

The moment-curvature and moment-deflection curves for specimens of series I and series II are shown in Fig. 3.



a) – self-stressed beams of the series I;
b) – self-stressed beams of the series II

Figure 3 – Relations «M-φ» and «M-a» obtained on the static loading stage

Test results obtained within loading of the self-stressed beams are listed in Table 6 and Table 7.

Table 6 – Failure modes and experimental value of cracking and ultimate loads obtained within self-stressed beams testing

Unit code	Cracking load (force) $P_{cr,c}$, kN ($M_{cr,c}$, kN·m)	Ultimate load (force) P_{ult} , kN (M_{ult} , kN·m)	Failure mode
I-BECS-(1)	34 (6,8)	108 (21,6)	«B»
I-BECS-(2)	37,3 (6,5)	120 (21,0)	
I-BECS-(3)	39,5 (6,9)	120 (21,0)	
I-BECS-(4)	46,6 (8,2)	125,4 (22,0)	
II-BECF-(1)	40,5 (8,1)	150 (30,0)	«Sh»
II-BECF-(2)	43,5 (8,7)	130 (26,0)	
II-BECF-(3)	39,0 (7,8)	150 (30,0)	

Note: «B» – flexural failure mode; «Sh» – shear failure mode.

Table 7 – Experimental values of the deflection and crack width obtained within self-stressed beams testing

Unit code	Deflection a , mm	Crack width (w_{max}/w_m), mm
I-BECS-(1)	2,3	0,1/0,1
I-BECS-(2)	2,7	0,15/0,07
I-BECS-(3)	2,9	0,1/0,09
I-BECS-(4)	3,2	0,1/0,1
II-BECF-(1)	4,9	0,7/0,59
II-BECF-(2)	4,6	0,6/0,38
II-BECF-(3)	4,6	0,6/0,47

Note: In the table values of deflections, maximum and average crack width correspond to the loading rate of $\approx 0,6 \cdot P_{ult}$, where P_{ult} – ultimate load.

For beams of series I and series II, the first cracks occurred in the pure bending region at the load of 44 kN (7,1 kN·m) and 41 kN (8,2 kN·m) on average, respectively. After that in case of FRP reinforced beams, the slope of moment-curvature (moment-deflection) curves showed considerable drop and it was kept almost constant up to failure, as it is shown in Fig. 3. In case of steel reinforced beams, three characteristic branch sections with different slopes was observed: the first branch section – up to cracking; the second branch section – from cracking and up to reinforcing steel yielding; the third branch section – from reinforcing steel yielding and up to the failure (see Fig. 3). With increasing of the bending moment up to 24 kN·m, in the FRP reinforced beams, multiple inclined flexural shear cracks occurred outside the pure bending region and extended to a distance approximately 20 mm from the top surface of the beam. When applied load reached 143,3 kN (28,7 kN·m) at average, diagonal tension flexural shear failure mode was reached, but to this time FRP reinforcing bars did not reach its ultimate tensile strains (in accordance with test results: $\epsilon_{rt,frp} = 0,933\%$). Taking into account that FRP reinforced self-stressed beams reinforcement ratio was equal to 1,6 % and 2,1 % for II-BECF-(1,2) and II-BECF-(3) respectively, that is considerably higher of the both balanced reinforcement ratio ($\rho_{bal} = 0,3\%$) and recommended in accordance with [9] reinforcement ratio $1,4 \cdot \rho_{bal} = 0,42\%$. For the real reinforcement ratio of the tested beams, expected failure mode is due to crushing of the concrete in compression, but an observed failure mode had changed on the flexural shear without crushing of the concrete in compression. Moreover, registered within testing value of the ultimate moment was at average in 2 times higher than predicted value of the ultimate moment in accordance with EN 1992-1-1 and based on the mean and established in tests values of the materials characteristics. In opposite to the FRP reinforced beams, failure mode and value of the ultimate load for steel reinforced self-stressed beams of series I was the same as it was predicted in accordance with EN 1992-1-1 (ratio between predicted and established within loading ultimate bending moments was equal to 0,90).

Characteristic modes of failure and crack patterns for beams of the both series I and series II are shown in the Fig. 4.

Based on the analysis of the obtained experimental results, it can be stated, that initial early age stress-strain state obtained on the expansion stage influenced on the beams behavior during loading. It was observed that for the

both series I and series II self-stressed beams cracking load was near 30 % from the ultimate load (see Table 6). Flexural cracks development through the concrete cross-section depth was following: raised flexural cracks extended on the average depth about 180 mm and 195 mm ($\approx 75\%$ from cross-section depth) for series I and series II beams respectively and saved this position almost up to the failure on the background of the gradually increasing cracks number and its opening. This effect is explained that in the self-stressed structures initial compressive stresses are saved in concrete under the crack. An observed cracks patterns in the member tensile zone (see Fig. 4) with an average distance between cracks 60 ± 15 mm indicated about practically uniform distribution of the stresses longwise reinforcing bars in tension that is inherent for pre-stressed structures.

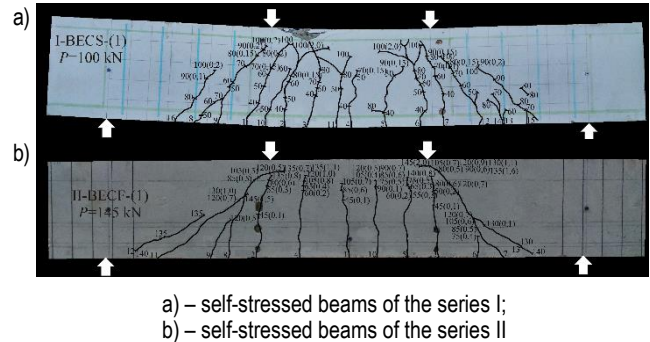


Figure 4 – General view of the beam crack patterns after test [16]

3.1.3 Diagram method comparison with experimental results

To analyze results obtained within static loading of the self-stressed beams with non-symmetric both FRP and steel reinforcement arrangement the « $M-\epsilon_{rt,x}$ » diagram was proposed (where M is a bending moment; $\epsilon_{rt,x}$ is a longitudinal tensile strain from the loading on depth of gravity center of the reinforcement in tension). The general view of the diagram is presented in the Fig. 5.

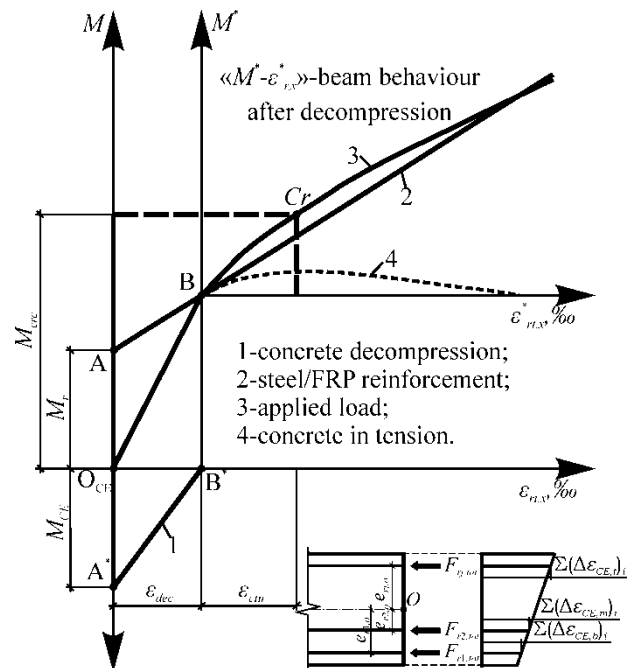


Figure 5 – Diagram for analysis of the initial stress-strain state influence on the behaviour under the loading of the non-symmetrically reinforced beams

Let us consider self-stressed beam under the monotonically increased load. Forces redistribution in the self-stressed beam cross-section under increasing load can be illustrated with the diagram presented in the Figure 1. Before load applying, in the beam cross-section balanced internal forces, obtained within self-stressing concrete expansion, are acting (see Fig. 1: $O_{CE}A = O_{CE}A^*$, $M_{CE} = M_r$). Moments from

the internal forces, accumulated to the end of the self-stressing stage, respectively concrete cross-section gravity center can be determined with respect to the value of the fixed restrained strains in reinforcement:

$$M_{CE} = M_r = \sum_{j=1}^n F_{rj,tot} \cdot e_{rj,o}, \quad (1)$$

where: M_{CE} and M_r are the balanced moments from self-stressing;

$e_{rj,o}$ – eccentricity of the force in the j -th restraint reinforcement

line respectively concrete cross-section gravity center;

$F_{rj,tot}$ – force in the j -th restraint reinforcement line, accumulated on the self-stressing stage to the concrete expansion stabilization that is determined as follows:

$$F_{rj,tot} = \varepsilon_{rj}(t_{tot}) \cdot E_r \cdot A_r, \quad (2)$$

where: $\varepsilon_{rj}(t_{tot})$ – strain in the j -th restraint reinforcement line, accumulated on the self-stressing stage to the concrete expansion stabilization, calculated in accordance with MSDM model [15-17];

E_r, A_r – modulus of elasticity and area of the restraint reinforcement respectively.

After applying and further monotonically increasing of the load, reducing of the initial concrete cross-section pre-compression, obtained on the self-stressing stage, was observed. Besides, up to decompression point B' (see diagram in the Fig. 5), cross-sectional tensile force is sustained by the reinforcement only (like it is in the traditional pre-stressed structures, line AB). Increment of the strains in reinforcement and increment of the bending moment, sustained by the reinforcement, before concrete decompression point B' is characterized by the AB line on the diagram in the Fig. 5. At the same time, reducing of the concrete initial compressive stresses corresponds to the internal moment changing along the A'B' line. At the point B' (see Fig. 5) concrete initial elastic compressive strains on the depth of gravity center of the reinforcement in tension reduces to 0 (so-called decompression stage). At the point B, line AB has the common point with the line O_{CE}B, characterized changing of the bending moment from the externally applied load. Within further loading after decompression point B', behavior of the self-stressed member is the same like behavior of the conventional RC-beam without any initial pre-stressing (part of the diagram in the « $M^* - \varepsilon_{rt,x}$ » axes). At this loading stage, a tensile force in concrete cross-section is sustained together by the concrete in tension and reinforcement right up to the flexural cracks appearing. Flexural cracks appear when tensile strains in concrete exceeds its ultimate values ε_{ctu} (see diagram in « $M^* - \varepsilon_{rt,x}$ » axes in the Fig. 5).

Thus, to the flexural cracks formation, the total strains respect to cracking $\varepsilon_{rt,cr}$ on the depth of reinforcement gravity center, is considered as a sum of decompression strains ε_{dec} and ultimate concrete tensile strains ε_{ctu} .

Resultant value of the cumulative concrete elastic strains $\varepsilon_{CE,el}(t_{sl})$, which corresponds to the decompression strains ε_{dec} at the static loading should be calculated as follows:

$$\varepsilon_{dec} = \varepsilon_{CE,el}(t_{sl}) = \frac{\varepsilon_{CE,eltot}(t_i) \cdot E_{c,aw}(t_i)}{E_{cm,sl}}, \quad (3)$$

where: $\varepsilon_{CE,eltot}(t_i)$ – concrete elastic strains accumulated to the end of the expansion stage and saved in structural member immediately before loading. It have to be calculated in accordance with proposed MSDM model [15-17];

$E_{c,aw}(t_i)$ – «average-weighted» expansive concrete modulus of elasticity, calculation procedure of it is presented in detail in [17];

$E_{cm,sl}$ – concrete modulus of elasticity to the static loading time;

t_i – age of concrete immediately before static loading.

Considering that decompression strains are a parameter that allows assessing the effectiveness of the initial self-stressing and to predict its further influence on the crack behavior of the beams, this parameter (ε_{dec}) was got from experimental results analysis with diagram « $M - \varepsilon_{rt,x}$ », using and compared with the total tensile strains immediately before cracking measured on the depth of the reinforcement gravity center $\varepsilon_{rt,cr}$.

This analysis of the self-stressing effectiveness was based on the assessment of the ratio between decompression strains ($\varepsilon_{dec,exp}$) and total tensile strains ($\varepsilon_{rt,cr}$), that is presented in Table 8.

Table 8 – Experimental values of the concrete tensile strains on the depth of the reinforcement gravity centre

Unit code	$\varepsilon_{dec,exp}$, ‰	$\varepsilon_{rt,cr}$, ‰	(2)/(3)
(1)	(2)	(3)	(4)
I-BECS-(1)	0,189	0,528	0,36
I-BECS-(2)	0,241	0,542	0,44
I-BECS-(3)	0,229	0,533	0,43
I-BECS-(4)	0,312	0,658	0,47
II-BECF-(1)	0,091	0,494	0,18
II-BECF-(2)	0,095	0,480	0,20
II-BECF-(3)	0,101	0,490	0,21

As it is shown in Table 8, from experimental research [17] this ratio was at average 0,43 and 0,20 for self-stressed beams of the series I and series II respectively.

For effectiveness of the FRP reinforcing bars application in the pre-stressed (self-stressed) structures, « $M - \varepsilon_{rt,x}$ » diagram was utilized (see Fig. 5). It was assessed from the experimental results, that before loading in the beams of Series I and Series II almost equal values of the moments created by the pre-compression forces was obtained (was at average 3 kN·m). Therefore decompression strains in case of FRP bars using were less approximately in two times in comparison with decompression strains registered in self-stressed beams with steel reinforcement (see Table 8). It was stated, that up to decompression point, resultant force in tensile zone of the cross-section is sustained by the reinforcing bars only (at this stage concrete is under the initial compressive stresses). Taking into account that steel and FRP bars are characterized by the different values of modulus of elasticity (FRP bars modulus of elasticity $E_{frpm} = 45,2$ GPa, that was close to the concrete modulus of elasticity $E_{cm} = 25,7$ GPa), a different values of the moment increment was observed for the same levels of the longitudinal tensile strains in reinforcement (in case of FRP reinforcement, such increments were sufficiently less). To obtain equal values of the moment increments in case of FRP and steel bars utilizing, required area of FRP reinforcement have to be increased considerably and can be found based on the optimization procedure (it consists in the assessment of the FRP reinforcement axial stiffness, that is necessary to provide desired values of the moment increments within decompression stage as well as initial self-stresses at the expansion stage).

Nevertheless, it should be pointed that obtained self-stressing parameters in the members reinforced with FRP bars not only lead to the cracking moment increasing, but change series II self-stressed beams post-cracking behavior. A number of cracks, comparable with cracks number in series I self-stressed beams with steel reinforcing bars was observed ($N=9$ and $N=12$ at average respectively), and maximum flexural crack width was not exceed 0,6 mm under the loading rate near $0,6 \cdot P_{ult}$.

2.2 Experimental studies [27]

2.2.1 Test specimens

Eight series of the self-stressed beams reinforced with FRP was tested in studies [27]. Beams in the experiment [27] were designed in such a way that they had asymmetric mixed reinforcement from steel and FRP bars near the bottom and top fiber of the section (see Fig. 6). However, despite different numbers and materials of reinforcement bars near the bottom and top fibres of the beam cross-section, their axial stiffness was very close ($A_s \cdot E_s = A_f \cdot E_f$).

Geometry, reinforcement arrangement and basic parameters of beams shown in Fig. 6.

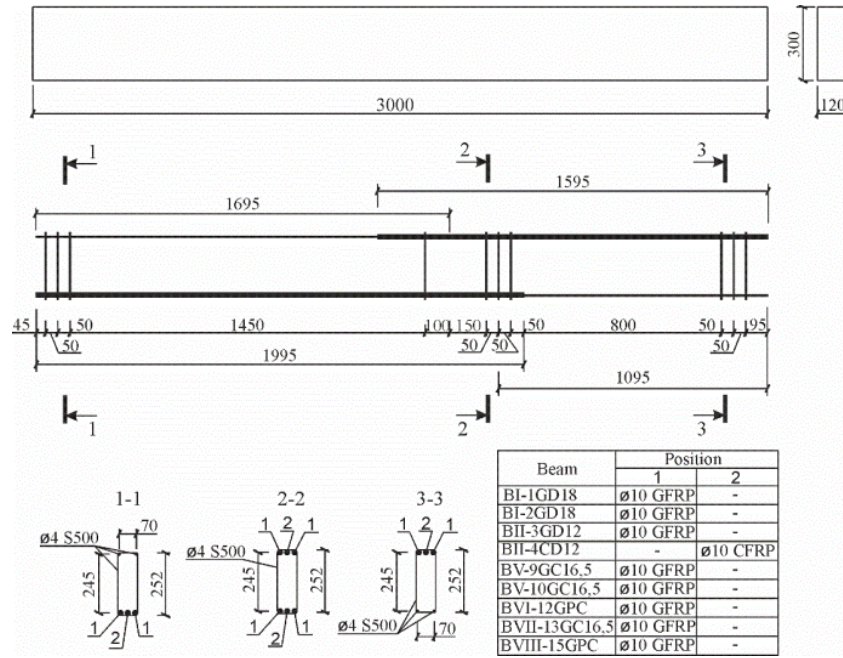


Figure 6 – Geometry, reinforcement arrangement and parameters of tested beams [27]

Expansive concrete mix nominal composition per 1 m³ of the beams of series BI-BII, BV-BVIII are listed in Table 9 [27].

Table 9 – Expansive concrete composition

Series	1 m ³ in dry conditions, kg					
	Cement	Denka CSA	Fine aggregate	Coarse aggregate	Water, l	Stachement 2010
BI	510	90	600	960	240	-
BII	410	50	805	990	175	7,0
BV, BVII	515	85*	740	880	201	7,5
BVI, BVIII	360	-	900	1060	148	5,4

Note: «*» – CSA 20.

Self-stressed beams of the series BI-BII, BV-BVIII were made of self-stressing concrete with characteristics presented in Table 10.

Table 10 – Average values of the self-stressing concrete characteristics

Series	Expansion characteristics at the concrete expansion stabilization		Mechanical characteristics	
	free expansion strain $\epsilon_{CE,f}$, %	reference self-stress $f_{CE,d}$, MPa	compressive strength $f_{cm,28}$, MPa	modulus of elasticity $E_{cm,28}$, GPa
BI	1,12	2,55	53,1	31,7
BII	0,02	0,45	76,5	43,3
BV	0,45	2,20	53,2	33,7
BVI	-	-	47,1	40,5
BVII	0,42	2,35	50,2	31,2
BVIII	-	-	30,7	32,1

Notes: 1. Free expansion strain, $\epsilon_{CE,f}$, was established on the unrestrained specimens;

2. Reference self-stress, $f_{CE,d}$, was established in the standard restraint conditions: $\rho=1\%$ and $E_s=200$ GPa;

3. Modulus of elasticity was established on the cylindrical specimens ($\varnothing=150$ mm, $h=300$ mm).

Steel and FRP reinforcing bars characteristics are listed in Table 11 and Table 12.

Table 11 – Mechanical characteristics of steel reinforcing bars (experimental values)

Nominal diameter, mm	Yield stress f_{ym} , MPa	Modulus of elasticity E_{sm} , GPa
4	573,2	200,0

Table 12 – Mechanical characteristics of FRP reinforcing bars

Nominal diameter, mm	Type of fibers	Modulus of elasticity E_{frpm} , GPa	Tensile strength f_{frpm} , MPa	Ultimate tensile strain ϵ_{frpm} , %
10*	Glass	40,8	760	2,0
10*	Carbon	155	2000	1,5
10**	Glass	32	1244	2,7

Note: «*» – this reinforcement was used in beams of the series BI-BII; «**» – this reinforcement was used in beams of the series BV, BVI-12GPC, BVII-13GC16,5 and BVIII-15GPC.

The measurement of the strains in the test beams at the stage of hardening and expansion of the self-stressing concrete underwater storage conditions was carried out using a strain meter with a digital indicator with a scale of 0.01 mm on a 270 mm basis (when measuring the deformations along the lateral face of the test beam). On each beam (series BI-BV) 4 strain meters are installed at the level of the reinforcement (in the middle sections of the span and cantilever part of the beam due to uneven reinforcement. On the beams of series BVII, two more strain meters are installed to study the process of self-stressing of concrete in a zone with the same reinforcement.

2.2.2 Results (self-stressing stage, expansive strains distribution)

Experimental values of the restrained strains at the level of reinforcement and self-stresses in concrete on the depth of the cross-section gravity center immediately before static loading are listed in the Table 13 and Table 14.

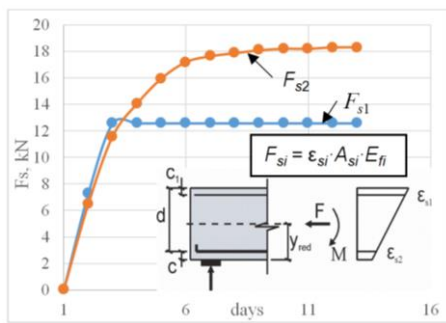
Table 13, 14 listed results of the measurement of the restrained strains on the level of the reinforcement, values of the calculated based on these strains tensile forces in reinforcement bars, and average self-stresses at the level of the center gravity of the section. Figures 7a,b show development in time tensile forces in restraint bars F_{s1} and F_{s2} near the top and bottom fibers of the cross-section respectively. We considered two series of beams performed from the self-stressing concrete with different values of standard self-stress grade in accordance with [...]. For beam BI-2SD18 from series BI standard self-stress was equal $f_{ce,m} = 2.55$ MPa, and for beam BV-9GC16,5 from series BV, it was equal $f_{ce,m} = 2.2$ MPa.

Table 13 – Experimental parameters of the self-stressing for beam BI-2GD18 (span)

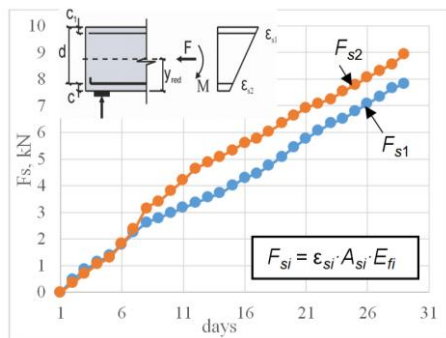
Days	$\epsilon_{s1} \cdot 10^{-5}$	$\epsilon_{s2} \cdot 10^{-5}$	F_{s1} , kN	F_{s2} , kN	F_o , kN	M_o , kNm	$\varphi_M \cdot 10^{-10}$, mm ⁻¹	$\varphi_\epsilon \cdot 10^{-5}$, mm ⁻¹	σ_{ce} , MPa
1	0	0	0	0	0	0	0	0	0
2	144,4	107,4	7,26	6,48	13,75	-0,11	-1,12	0,15	0,38
3	283,3	192,6	12,57	11,61	24,2	-0,14	-0,62	0,37	0,67
4	355,6	233,3	12,57	14,07	26,62	0,15	0,44	0,50	0,74
5	413	264,8	12,57	15,97	28,49	0,38	0,88	0,61	0,79
6	438,9	285,2	12,57	17,2	29,71	0,53	1,05	0,63	0,83
7	450	292,6	12,57	17,64	30,15	0,58	1,03	0,65	0,84
8	453,7	296,3	12,57	17,87	30,37	0,61	1,0	0,65	0,84
9	457,4	300	12,57	18,09	30,59	0,63	0,97	0,65	0,85
10	459,3	301,9	12,57	18,2	30,7	0,65	0,96	0,65	0,85
11	461,1	301,9	12,57	18,2	30,7	0,65	0,92	0,66	0,85
12	461,1	303,7	12,57	18,31	30,81	0,66	0,91	0,65	0,86
13	463	303,7	12,57	18,31	30,81	0,66	0,89	0,66	0,86

Table 14 – Experimental parameters of the self-stressing for beam BV-9GC16,5 (span)

Days	$\epsilon_{s1} \cdot 10^{-5}$	$\epsilon_{s2} \cdot 10^{-5}$	F_{s1} , kN	F_{s2} , kN	F_o , kN	M_o , kNm	$\varphi_M \cdot 10^{-10}$, mm ⁻¹	$\varphi_\epsilon \cdot 10^{-5}$, mm ⁻¹	σ_{ce} , MPa
1	0	0	0	0	0	0	0	0	0
2	9,3	7,4	0,47	0,35	0,82	-0,02	-0,11	0,008	0,02
3	16,7	14,8	0,84	0,70	1,54	-0,02	-0,06	0,008	0,04
4	22,2	22,2	1,12	1,05	2,17	-0,01	-0,02	0	0,06
5	27,8	27,8	1,40	1,31	2,71	-0,01	-0,02	0	0,08
6	36,1	38,9	1,81	1,84	3,65	-0,001	-0,002	-0,01	0,10
7	44,4	50,0	2,23	2,36	4,59	0,01	0,02	-0,02	0,13
8	51,9	66,7	2,61	3,15	5,76	0,06	0,09	-0,06	0,16
9	55,6	72,2	2,79	3,41	6,20	0,07	0,10	-0,07	0,17
10	59,3	80,6	2,98	3,81	6,78	0,09	0,12	-0,09	0,19
11	63,0	88,9	3,17	4,20	7,36	0,12	0,16	-0,11	0,20
12	66,7	98,1	3,35	4,64	7,98	0,15	0,19	-0,13	0,22
13	70,4	102,8	3,54	4,86	8,39	0,15	0,19	-0,13	0,23
14	74,1	107,4	3,72	5,08	8,79	0,16	0,20	-0,14	0,24
...									
29	155,6	188,9	7,82	8,93	16,74	0,12	0,13	-0,14	0,47



a)



b)

a) – beam BI-2GD18 (span); b) – beam BV-9GC16,5 (span)

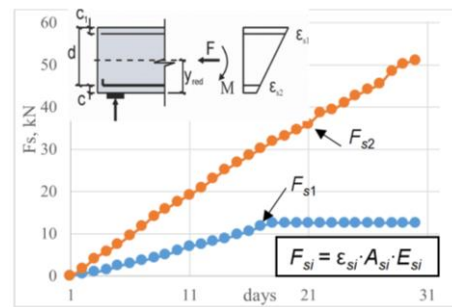
Figure 7 – Development of the tensile force in reinforcement at the expansion stage

As shown from Figure 7 for different reinforcement ratios near the top and bottom fibres of cross-section, but the very close value of the bars axial stiffness, the tensile forces in steel and FRP bars increased practically the same before expansion stabilization. At the stage of the expansion stabilization, the beam practically does not deflect (the value of the curvature is equal $\varphi_{ce} = 1,4 \cdot 10^{-6} \text{ mm}^{-1}$). The average value of the self-stress at the level of the center gravity of the cross-section was equal to 0.47 MPa (see Table 14 and Fig. 7b). Some different behavior at the expansion stage of the expansive concrete we can observe for beam BI-1GD18.

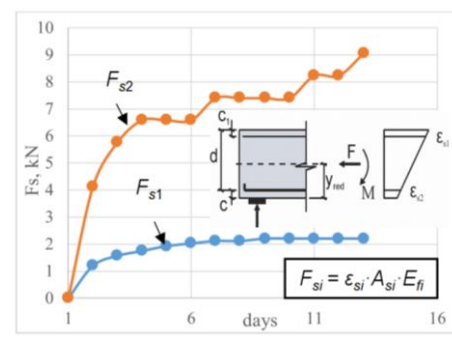
At the initial stage of expansion (near 2 days) the values of restrained strains and tensile forces in reinforcement, respectively, developed practically the same. However, at 3-day age restraint strain in steel reinforcement ($\varnothing 4 \text{ S500}$) exceeded yield strain for steel ($\epsilon_{s1} = 2,83\text{‰} > \epsilon_{sy} = 2,17\text{‰}$). After that increasing of restrained strain does not provide to increasing of the tensile force in steel reinforcement (see Fig. 7a and Table 13) and this force remains practically constant $F_{s1} = f_y \cdot A_s$.

As a result, the main restraint element becomes FRP bars and additional tensile force is developed now in these bars. Because the difference in the values of the restrained strains at the level the top and bottom reinforcement took place the beam was deflected (the value of the curvature was equal $\varphi_{ce} = 6,6 \cdot 10^{-6} \text{ mm}^{-1}$), but sections remain plain.

Comparison with results obtained by testing the beams reinforced with steel reinforcement only (beams BIV-8SC16,5 and BIII-SD15) shows that, because axial stiffness of the bars near opposite fibres of section differs sufficiently, we can observe differences in the development of the axial tensile forces (see Fig. 8). Tensile forces in the bottom steel bars $\varnothing 12 \text{ S500}$ increased practically linearly before the self-stressed concrete expansion strain stabilization. In the top reinforcement bars $\varnothing 4 \text{ S500}$ at 17 days, tensile strains exceeded steel yielding strains ($\epsilon_{s1} = 2,33\text{‰} > \epsilon_{sy} = 2,17\text{‰}$) and tensile force stabilized at the level $F_{s1} = f_y \cdot A_s$. The average self-stress value at the level of centre of gravity of section was equal to 1,7 MPa. The curvature of the beam now of expansion stabilization was equal $\varphi_{ce} = 19,2 \cdot 10^{-6} \text{ mm}^{-1}$ (for comparison curvature $\varphi_{ce} = 6,6 \cdot 10^{-6} \text{ mm}^{-1}$ for the beams reinforced by FRP).



a)



b)

a) – beam BIV-8SC16,5 (span); b) – beam BIII-6SD15 (span)

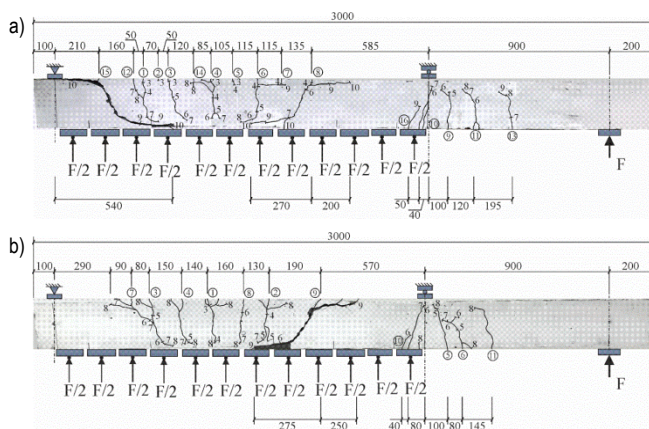
Figure 8 – Development of the tensile force in reinforcement at the expansion stage

As with experiments [27], induced self-stresses influenced the shear resistance of the tested beams under uniformly distributed loads. Table 15 listed experimental results of the load testing of the self-stressed beams reinforced with FRP and beams performed from OPC-concrete reinforced with FRP too. Crack patterns after testing the beams are shown in Figure 9. The forces registered during static tests, corresponding to the formation of cracks and the ultimate forces, are presented in Table 15.

Table 15 – Results of static tests under the action of a uniformly distributed load in the span of a beam

Series	Beam	P_{cr} kN	q_{cr} kN/m	P_u kN	q_u kN/m	Mode of failure
BI	BI-1GD18 (without loading the cantilever)	-	29,6	-	87,3	Diagonal crack
	BI-2GD18	10,4	34,7	22,5	75,0	Diagonal crack in the span
BII	BII-3GD12	10,4	34,7	24,5	81,7	Diagonal crack in the cantilever
	BII-4CD12	8,4	28,0	24,5	81,7	--/--
BV	BV-9GC16,5	6,4	21,3	20,2	67,5	Diagonal crack in the span
	BV-10GC16,5	6,4	21,3	18,5	61,6	Diagonal crack in the cantilever
BVI	BVI-12GPC	6,4	21,3	18,2	60,6	Diagonal crack in the span

Notes: 1. P_{cr} – point force applied in the cantilever, corresponding to cracking;
2. q_{cr} – uniformly distributed load applied in the span of a beam corresponding to cracking;
3. P_u – point force applied in the cantilever, corresponding to failure;
4. q_u – uniformly distributed load applied in the span of a beam corresponding to failure.



a) – BV-9GC16,5 (expansive concrete); b) – BVI-12GPC (opc-concrete)

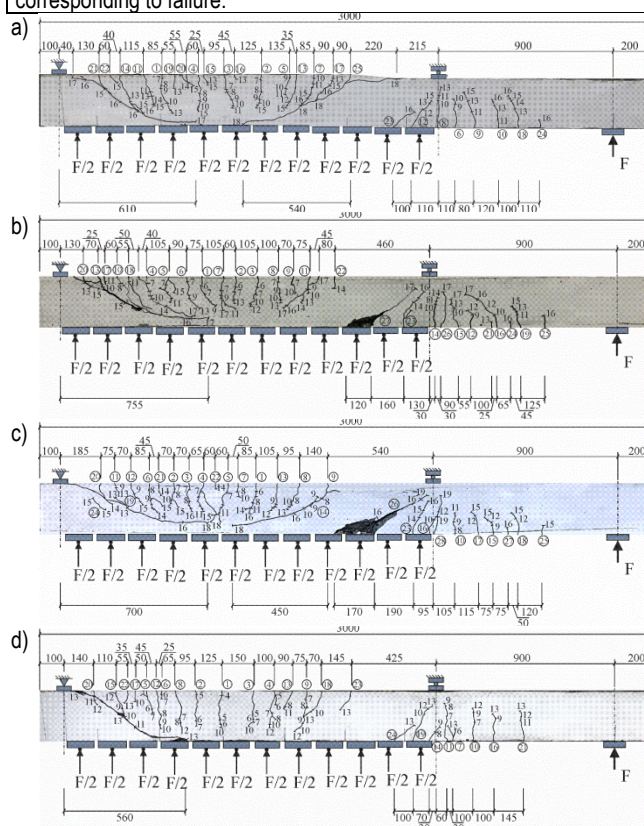
Figure 9 – Cracks patterns for tested beams

Initial self-stresses now of the expansion stabilization for beams series BV was equal ≈ 0.47 MPa, and was partially compensated by shrinkage in the time before testing. So cracking loads for self-stressed beams BV-9GC16,5 and BV-10GC16,5 practically was the same as the cracking loads registered for beams performed from OPC-concrete (beam BVI-12GPC). However, for the beam series BII, cracking loads were on 31 % (beam BII-4CD12) and 62.5 % (beams series BI and BII-3GD12) greater than for beams performed from OPC-concrete. Analogical results were obtained for beams reinforced with steel bars. For the beams (series BIV) cracking loads were on 48 % and for the beam BIII-6SD15 even on 72 % greater than for the analogical beams performed from OPC-concrete (beam BVI-11SPC) (see Table 16). The cracks development and final crack pattern depend on the achieved value of self-stressing after failure (see Fig. 10). For self-stressed beams reinforced with steel bars and FRP bars, the cracks development and final crack pattern depend on the achieved value of self-stressing after failure.

Table 16 – Results of static tests under the action of a uniformly distributed load in the span of a beam

Series	Beam	P_{cr} kN	q_{cr} kN/m	P_u kN	q_u kN/m	Mode of failure
BIII	BIII-6SD15	14,5	48,2	36,6	122,1	Diagonal crack in the span
BIV	BIV-7SC16,5	12,4	41,4	34,6	115,3	--/--
	BIV-8SC16,5	12,4	41,4	37,9	126,3	--/--
BVI	BVI-11SPC	8,4	28,0	26,5	88,5	--/--

Notes: 1. P_{cr} – point force applied in the cantilever, corresponding to cracking;
2. q_{cr} – uniformly distributed load applied in the span of a beam corresponding to cracking;
3. P_u – point force applied in the cantilever, corresponding to failure;
4. q_u – uniformly distributed load applied in the span of a beam corresponding to failure.



a) – BIII-6SD15 (expansive concrete);
b) – BIV-7SC16,5 (expansive concrete);
c) – BIV-8SC16,5 (expansive concrete); d) – BVI-11SPC (opc-concrete)

Figure 10 – Cracks patterns for tested beams

The behavior of the self-stressed beams reinforced with FRP at the ultimate limit state needs a separate analysis and does not subject to this paper.

Conclusions

What can we conclude from the results of the presented experimental and theoretical investigations?

- (1) A self-stressed structure -is a pre-stressed structure, in which we create the tension of the reinforcement by the work that self-stressing concrete performs against restraint at the expansion stage. Resultant pre-stressing force transfers from tendons to expanding concrete by the bond or anchorage and depends on the degree of restraint. The cases considered are those when misalignments are not produced at the respective contact surface between expansive concrete and reinforcing bars.

- (2) Independently from the type of restraint (steel bars or FRP bars) transferring of the chemical pre-stressing force to self-stressing concrete is realized like for traditional pre-stressed structure. At all stages of the self-stressing expansive strains are linearly distributed in the direction of the cross-sectional height. Considering, that self-stresses distribution is related to the restrained strain distribution, I can not imagine why such local stress distribution was adopted by Boxing Wang as a basic assumption in the "theory of self-stressing distribution model" [11], and repeated in a more controversial form as an assumption to "calculation model of cracking load and deflection of textile reinforced self-stressing concrete" [10].
- (3) Self-stressing is related to the elastic part of deformations only. All rules applied to the design of the pre-stressed structures (for checking of the serviceability limit states) are valid for self-stressed structures reinforced with FRP. In such a case, why do we have to apply the finite difference method for the calculation of cracking load and deflection of TRSSC beams? According to the modern crack resistance theory cracking load depends mainly on the ultimate tensile strain of concrete (no tensile strength). Based on the obtained test results authors [10] conclude that "the comparison of calculated and test values indicates an error of less than 30%, which is consistent with each other, thus verifying the applicability of calculation method". It is a very optimistic statement!

The following conclusion is optimistic too: "self-stress can significantly improve the cracking resistance of TRSSC beams. Although the tensile strength of the matrix of TRSSC is 26.07% lower than that TCR, the cracking loads of the TRSSC beam are increased by 33.39% and 30.29%". In first, in the experiment self-stressing cement grade 4.0 (self-stress in standard condition is equal to $f_{ct,m} = 4.0$ MPa) was used. Matrix specimens were cured before tensile testing in non-restrained conditions. In such conditions unbalanced expansion of the active self-stressing cement matrix, leads to self-damaging of the own material structure and decreasing of the tensile (and compressive) strength. Testing these specimens after curing in the restrained conditions (as if it was in tested prisms) will get higher values of the tensile strength. Now it is difficult to assess what is the value of tensile strength we have to account for when we want to verify the proposed crack resistance model. Moreover, experimental results presented in [10,11] are very unclear and non-representative. For instance, the same mix proportions for matrix type NC and SSC; dimensions of the reinforced TRSSC beams (prisms 100x100x400mm for testing so sensitive parameter as crack resistance); measurement (with unknown error) of the longitudinal deformations with the usage of the laser rangefinder only at the level of the layer of textile; curing under standard conditions, etc.)

At the finish of this paper, I want to point out there one of my impressions and write one curt remark. I always considered the CBM journal as a very serious and high-level edition and publication in this journal was a great honor...

References

- Peligot, E.-M. Bulletin Societe d'Encougrament pour L'Industrie Nationale / E.-M. Peligot, C. A. Gagout. – Paris : Incentive Company for the Development of National Industry, 1890. – Vol. 5. – P. 682.
- Michaelis, W. Tonindustrie-Zetung (Goslar). – 1892. – Vol. 16. – P. 105.
- Lossier, H. Expanding Cements and Their Application- Self-stressed concrete / H. Lossier, A. Gagout // Le Genie Civil (Paris). – 1944. – Vol. 121. №8, April 15. – P. 61–65.
- Mikhailov, V. V. Stressing Cement and the Mechanism of self-stressing concrete regulation / V. V. Mikhailov // Proceeding of IV Symposium Chemistry of Cement. – 1960. – Washington. – P. 134.
- Mikhailov, V. Expansive and self-stressing cement and self-stressed reinforced structures / V. Mikhailov, S. Litver. – Moscow : Stroyizdat, 1974. (in Russian)
- Mather, B. Expansive cement / B. Mather // Miscellaneous paper C-7-21, National Technical Information Service. – 1970.
- Klein, A. Studies of Calcium Sulfoaluminate Admixtures for Expansive Cement / A. Klein, A. Troxell // ASTM. – 1958. – Vol. 58. – P. 968–1008.
- Metha, P. K. Formation of Ettringite by Hydration of System Containing an Anhydrous Calcium Sulfoaluminate / P. K. Metha, A. Klein // Journal ACI. – 1965. – P. 435–436.
- Guttman, P. V. Expansive cement in USA / P. V. Guttman // ASCE. – 1967. – Vol. 37. № 11. – P. 135.
- Calculation method of cracking load and deflection of textile reinforced self-stressing concrete / B. Wang [et al.] // Construction and Building Materials. – 2021. – № 304. – 124622. – DOI: 10.1016/j.conbuildmat.2021.124622.
- Wang, B. Distributed models of self-stress value in textile reinforced self-stressing concrete / B. Wang, J. Zhao, Q. Wang // Construction and Building Materials. – 2016. – № 126. – P. 286–296. – DOI: 10.1016/j.conbuildmat.2016.06.149.
- Man, T. Expansion behaviour of self-stressing concrete confined by glass-fiber composite meshes / T. Man, B. Wang, H. Jin, X. Zhang // Construction and Building Materials. – 2016. – № 128. – P. 38–46. – DOI: 10.1016/j.conbuildmat.2016.10.022.
- He, H. Performance of steel fiber reinforced self-stressing concrete / H. He, B. Wang, J. Lin // Key Engineering Materials. – 2009. – № 400–402. – P. 427–432. – DOI: 10.4028/www.scientific.net/KEM.400-402.427.
- Tsuji, Y. Methods of estimating chemical prestress and expansion distribution in expansive concrete subjected to uniaxial restraint / Y. Tsuji // Concrete Library of JSCE. – 1984. – № 3. – P. 131–143.
- Tur, V. Self-stressed concrete members reinforced with FRP bars / V. Tur, M. F. Herrador, V. Semianiuk // Proceeding of the fib Symposium. – 2017. – P. 431–438.
- Semianiuk, V. Crack resistance of self-stressed members reinforced with FRP bars / V. Semianiuk, V. Tur // Solid state phenomena. – 2018. – № 272. – P. 244–249. – DOI: 10.4028/www.scientific.net/ssp.272.244.
- Early age strain and self-stresses of expansive concrete members under uniaxial restraint conditions / V. Semianiuk [et al.] // Construction and building materials. – 2017. – № 131. – P. 39–49.
- Scheerer, S. Textile reinforced concrete – from the idea to a high performance material / S. Scheerer, F. Schladitz, M. Gurbach // 11th International symposium on ferrocement and textile reinforced concrete, 3rd ICTRC. – 2015. – P. 15–33.
- Mather, B. Expansive cement / B. Mather // Miscellaneous paper C-7-21, National Technical Information Service. – 1970.
- Wang, V. Prediction of expansion behaviour of self-stressing concrete by artificial neural networks and fuzzy inference systems / V. Wang, T. Han, H. Jin // Construction and Building Materials. – 2015. – № 84. – P. 184–191.
- TCP 45-5.03-158-2009. Concrete and reinforced concrete structures from self-stressing concrete: design rules. – Minsk, 2010. (in Russian)
- Ishikava, Y. Initial stress analysis of expansive material under restrictions based on chemical conservation law / Y. Ishikava, K. Shibata, T. Tanabe // Creep, shrinkage and durability mechanics of concrete and concrete structures. – 2009. – P. 437–443.
- Early age deformation and resultant induced stress in expansive high strength concrete / H. Ito [et al.] // Journal of Advanced Concrete Technology. – 2004. – № 2 (2). – P. 155–174.
- Zdanowicz, K. Chemical prestress on concrete with carbon textile reinforcement: Theoretical and analytical approaches / K. Zdanowicz, S. Marx // Proceedings of the fib Symposium. – 2019. – P. 259–265.
- STB 2101-2010. Self-stressing concretes: specifications. – Minsk, 2011. (in Russian)
- He, H. Research of long-term expansive deformation of stress fiber reinforcement self-stressing concrete / H. He, J. Qin, C. Huang // Journal of building materials. – 2009. – № 12 (5). – P. 595–598.
- Varabei, A. Experimental studies of the resistance shear of self-stressed concrete beams under different loading conditions / A. Varabei, V. Tur // Vestnik PSU, Series F. – 2021. (in Russian)
- Guide for self-stressed concrete structures design SN-511. – P. 32. (in Russian).

Accepted 19.11.2021